

Using Features at Multiple Temporal and Spatial Resolutions to Predict Human Behavior in Real Time^{*}

Liang Zhang¹[0000-0002-1966-0864], Justin Lieffers¹[0000-0003-4527-8850], and Adarsh Pyarelal¹[0000-0002-1602-0386]

University of Arizona, Tucson AZ 85721, USA
{liangzh, lieffers, adarsh}@email.arizona.edu

Abstract. When performing complex tasks, humans naturally reason at multiple temporal and spatial resolutions simultaneously. We contend that for an artificially intelligent agent to effectively model human teammates, i.e., demonstrate computational theory of mind (ToM), it should do the same. In this paper, we present an approach for integrating high and low-resolution spatial and temporal information to predict human behavior in real time and evaluate it on data collected from human subjects performing simulated urban search and rescue (USAR) missions in a Minecraft-based environment. Our model composes neural networks for high and low-resolution feature extraction with a neural network for behavior prediction, with all three networks trained simultaneously. The high-resolution extractor encodes dynamically changing goals robustly by taking as input the Manhattan distance difference between the humans' Minecraft avatars and candidate goals in the environment for the latest few actions, computed from a high-resolution gridworld representation. In contrast, the low-resolution extractor encodes participants' historical behavior using a historical state matrix computed from a low-resolution graph representation. Through supervised learning, our model acquires a robust prior for human behavior prediction, and can effectively deal with long-term observations. Our experimental results demonstrate that our method significantly improves prediction accuracy compared to approaches that only use high-resolution information.

Keywords: Theory of Mind · Urban search and rescue · Neural networks.

^{*} This research was conducted as part of DARPA's Artificial Social Intelligence for Successful Teams (ASIST) program, and was sponsored by the Army Research Office and was accomplished under Grant Number W911NF-20-1-0002. The views and conclusions contained in this document are those of the authors and should not be interpreted as representing the official policies, either expressed or implied, of the Army Research Office or the U.S. Government. The U.S. Government is authorized to reproduce and distribute reprints for Government purposes notwithstanding any copyright notation herein.

1 Introduction

Artificially intelligent (AI) teammates should have a number of capabilities to be effective [1], including inferring the internal states of other agents [2–4], solving problems collaboratively with them [5–7], and communicating with them in a socially-aware manner [8,9]. While these capabilities have been developed to some extent for simple domains (e.g., 2D gridworlds) and simulated agents, current state of the art approaches still face significant challenges when it comes to dealing with complex domains and modeling actual human teammates (as opposed to simulated agents). We attempt to address some of these challenges in the context of an experiment involving humans conducting a simulated urban search and rescue (USAR) mission set in a Minecraft-based environment [10].

This domain is significantly more complex than the domains previously studied in the literature on computational theory of mind (ToM) [2,3]. Enabling AI agents to understand human behavior in complex domains will be essential to achieve the goal of better human-AI teaming. The complexity of the domain and the emphasis on analyzing human subjects lead to a few unique challenges, which we describe below.

- **Limited data.** Since collecting human subjects data is expensive and time-consuming, the amount of training data available to us is very limited. This rules out using certain classes of modern machine learning approaches (e.g., transformer architectures) that require a large amount of training data.
- **Noisy data.** Human subjects data is typically noisy, especially in the short term, with participants frequently violating assumptions of rationality that are used in existing works on computational ToM [2,3,11]. This expresses the need for a two resolution approach as rationality can often be recovered when the domain is represented at a lower resolution and the noise is averaged over, yet the high resolution is required for real-time predictions.
- **Long horizon.** In contrast to earlier works on computational ToM [2,3,11] that study domains with $\approx 10^2$ primitive actions per episode¹, our work considers a domain with episodes containing $\approx 10^3$ primitive actions and a far larger observation space including more than 20 areas and complex connectivity. This requires us to implement a long-term memory mechanism and the ability to extract key features from large amounts of noisy data, both of which are challenging in their own right.
- **Complex dynamics.** Our domain is large and possesses a complex topological structure, coupled with a complex rescue mechanism setting (for details, please refer to the approach section), which require us to consider human behavior at different levels of spatial and temporal granularity. Our model simultaneously takes into account both the *short-term goal preference* in a local area and the *long-term rescue strategy*.

¹ We use the term *episode* to denote a sequence of actions taken by an agent to perform a given task. We also use the term *trial* elsewhere in the paper to denote the same thing.

To address the above challenges, we propose a two-level representation. The first is a *low-resolution* level that contains information about the topology of the environment (i.e. which areas are connected to each other) and the status of victims in each area. The second is a *high-resolution* level that contains more granular information about the environment, such as the Cartesian coordinates corresponding to the agent’s current location, walls, openings, and victims inside the rooms.

For the low-resolution representation, we build a matrix that encodes key historical information, which helps our model learn high-level features of human behavior, such as long-term search and rescue strategies. In contrast, for the high-resolution representation, we organize the input vector to our proposed model based on the latest short-term observations, which are more conducive to recognizing short-term goal preferences. Using the high and low level resolutions simultaneously aligns with the way humans reason about complex tasks, and also results in better performance on our prediction tasks, compared to considering only a single resolution.

2 Related Work

There exist a number of other approaches to computational ToM in the literature. In this section, we describe some of them, along with their advantages and disadvantages compared with our approach.

Bayesian Theory of Mind (BToM) models [3,12,13] calculate the probabilities of potential goals of an agent and other’s beliefs. These models are primarily based on Markov Decision Process (MDP) formalisms and thus suffer from high computational costs for complex domains.

Zhi-Xuan et al. [11] proposed an online Bayesian goal inference algorithm based on sequential inverse plan search (SIPS). This approach allows for real-time predictions on a number of different domains. Notably, their approach models agents as *boundedly rational planners*, thus making them capable of executing sub-optimal plans, similar to humans. However, this approach cannot be directly applied to our domain due to the fact that our agents (i.e., humans) have incomplete knowledge of their domain and thus the short term planning would suffer without added hierarchical complexity or longer term planning. In our proposed approach, we use a similar idea of calculating the probabilities of potential goals, but we use neural networks which allow for the automatic extraction of features and correlations from the data without having to hand-craft conditional probability distributions.

Our supervised learning approach considers both long-term historical and real-time high-resolution features in a robust fashion, dramatically reducing the computational costs of training and deployment in online settings even for complex domains.

Inverse reinforcement learning (IRL) methods [14–17] make real-time predictions about an agent from learning the agent’s reward function by observing its

behavior. However, IRL methods suffer in online settings for complex domains because they are based on MDP formalisms, similar to BToM approaches [18,19].

Approaches based on plan recognition as planning (PRP), which use classical planners to predict plan likelihoods given potential goals, can also give real-time predictions for complex domains [20–25]. However, these methods require labor-intensive manual knowledge engineering, which can be prohibitive for environments that have complex dynamics. Additionally, these methods struggle with the noisy and sub-optimal nature of human behavior. In contrast, our neural network based approach requires minimal manual knowledge engineering and our two levels of resolutions allow for an effective treatment of noisy/sub-optimal behavior.

Guo et al. [26] study the same domain as the one in this paper, and use a graph-based representation for their model as well. However, they focus on transfer learning as a way to improve training when dealing with a limited amount of training data. Additionally, their agent predictions are focused on navigation. The techniques developed in their work are applicable to us and could be useful to further expand our model in the near future.

Lastly, Rabinowitz et al. [2] used meta-learning to build models of the agents from observations of their behavior alone. This resulted in a prior model for the agents’ behavior and allowed for real-time predictions. However, this approach only studied situations where the agents followed simple policies, and the dynamics of their domain are much simpler than ours.

3 Approach

3.1 Domain and task

The domain we consider is that of a USAR mission simulated in a Minecraft-based environment [10]. In this scenario, the participants must navigate an office building that has suffered structural damage and collapse due to a disaster. The original building layout is altered by the collapse, with some passages being closed off due to rubble, and new openings being created by walls collapsing.

The goal of the mission is to obtain as many points as possible by triaging victims of the building collapse within a 10-minute time limit. There are 34 victims in the building, among whom 10 are seriously injured and will expire 5 minutes into the mission. These *critically injured* victims take 15 seconds to triage and are worth 30 points each. These victims are represented by *yellow* blocks. The other victims are considered *non-critically injured*, take 7.5 seconds to triage, and are worth 10 points each. These victims are represented by *green* blocks.

Each participant conducts three versions of the mission, with different levels of difficulty (easy, medium, and hard). On higher difficulty levels, the victims are less clustered, further away from the starting point, and are more difficult to find. Higher difficulty levels also have more alterations from the original static map that the participants are provided at the beginning of the mission (i.e., more blockages and openings).



Fig. 1. A visualization of the high-resolution representation for our domain. The red dot represents the agent (i.e., the human’s Minecraft avatar), and the grey dots represent grid cells that the agent has traversed in the past. Green and yellow squares represent untriated victims, blue squares represent triaged victims, brown squares represent walls, and grey squares represent obstacles. Walls and obstacles are not traversable, and the blank (white) squares are walkable areas.

3.2 Representation

High-Resolution Representation We use a highly simplified 2D gridworld environment representation for the high resolution representation. In this representation, we encode different objects and store them in a 51×91 integer matrix. The specific encodings are shown in Table 1.

Table 1. Encodings for objects in the high resolution representation.

Object	Value
Empty	1
Wall	4
Critical victim	81
Non-critical victim	82
Unavailable victim (triaged or expired)	83
Obstacle	255
Agent	0

In Fig. 1, we show a visualization of the high-resolution representation². Our primitive action space consists of two types of actions: *move* and *triage*. The

² Our high-resolution visualization code implementation is based on this repository: https://gitlab.com/cmu_asist/gym_minigrid

‘move’ action can be carried out in four directions: up, down, left, and right, moving one cell at a time when the direction of moving is not obstructed. The ‘triage’ action can only be performed when the agent reaches locations cells where victims are located.

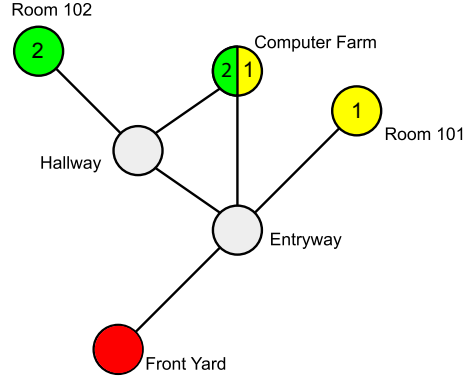
In this high-resolution representation, we can analyze human behavior based on discrete primitive actions combined with the layout of the building, which enables modeling real-time changes in short-term goal preferences. However, these actions also introduce noise, and inference based on them alone is not conducive to extracting high-level features and organizing long-term memory due to the large number of primitive actions per trial ($\approx 10^3$).

Low-Resolution Representation To facilitate the extraction of high-level features from human behavior and the organization of long-term historical information, we construct a graph-based representation to simplify our domain further. The nodes of the represent areas (e.g., rooms, hallways, etc.) of the building, the edges represent connections between areas, and each node has three integer-valued attributes:

- Number of green victims in the area.
- Number of yellow victims in the area.
- Visited status. This attribute can take one of four possible values:
 - 0: The node has not been previously visited by the agent.
 - 1: The node has been previously visited by the agent.
 - 2: The agent is currently located at the node.
 - 3: The node was the previous node the agent was at.

For ‘visited status’ attribute, if two conditions are met at the same time, the higher encoding value has a higher priority. For example, if the agent returns to a previously visited room, the visited status of the current room defaults to 2 instead of 1 even though both are applicable. The visited status in the memory matrix is updated according to the above rules when the agent moves from one area to the next. In addition, when the agent successfully triages a specific type of victim, the number of victims of that type in the current area is reduced by one. Therefore, the updates to this matrix record the historical behavior of the current agent.

This is a dramatic simplification of our domain, since we ignores many details from the environment, such as the specific locations of agents and victims, the detailed layout of the building, etc. Therefore, the low-resolution representation provides a more concise encoding of crucial historical information, making it easier for the model to extract high-level features in human behavior. We organize this information into a matrix. However, the time interval for state updates is longer than that in the high-resolution representation, since we are not encoding primitive actions for this representation, and it cannot grasp real-time changes in human intentions. Figure 3 shows an example sketch of the time intervals for updates to the state in the two resolutions. In order to leverage the complementary strengths of these two resolutions, we propose a model that uses both as inputs simultaneously.



Area ID	Yellow victims	Green victims	Visited status
Room 101	1	0	0
Room 102	0	2	1
Front Yard	0	0	2
Entryway	0	0	3
Hallway	0	0	1
Computer Farm	1	2	0

Fig. 2. Visualization of an example low resolution graph representation and the corresponding memory matrix. The nodes represent the areas in the building, and the edges the connections between them. The number and type of victims in each area are recorded as attributes on each node, and are shown using a color and number indicating the type and quantity of victims. The red node represents the node the agent is in. The matrix below the graph is the corresponding low resolution memory matrix.

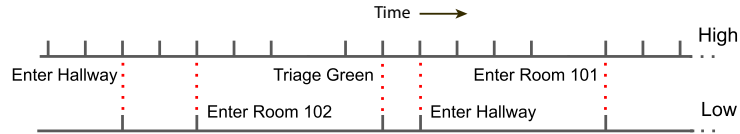


Fig. 3. An example sketch showing the different time intervals of state updating for the two resolutions. Each tick line indicates an update to the state, and the red dotted lines connect ticks with the same timestamp. The high resolution input is updated for every primitive action, while the low resolution input is only updated when the agent leaves a node or changes the attributes of a node (triaging a victim), hence the lesser number of ticks.

3.3 Model

Our model produces two types of outputs: (i) *goals*, i.e., objects/locations that the agent is trying to get to, and (ii) the *next type of victim* (green or yellow) that the agent will attempt to triage.

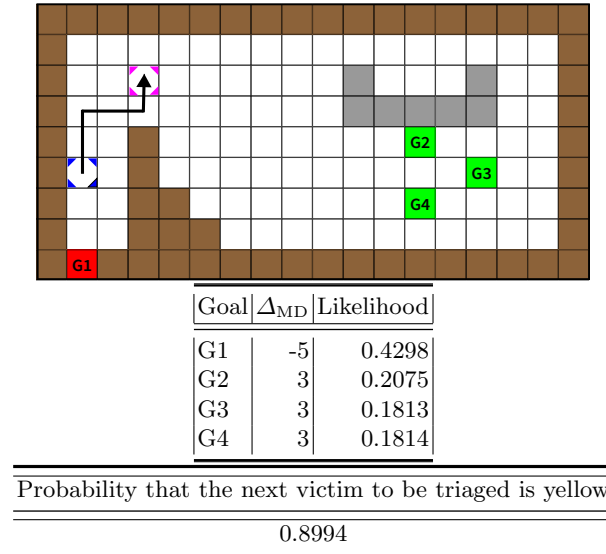


Fig. 4. An example of how we deal with the data from the high resolution representation. The arrows represent the agent’s last six movements. The quantity $\Delta_{MD}(g, 6)$ (see eq. 1) is computed for $g \in \{G1, G2, G3, G4\}$ and shown in the table below the figure, along with the predictions of the model for each potential goal g in the area. The window of ‘move’ actions is from when the agent moves from the magenta outlined square to the blue outlined square.

Goals The primary outputs of our model are similar to methods based on Bayesian ToM approaches [3, 12, 13]. We consider victims and portals connecting adjacent areas as potential goals, and aim to predict which goal the agent is currently pursuing. See Figure 4 for an example set of goals available to an agent when entering a particular room.

Next Triageed Victim Type In addition to predicting the probability of the agent pursuing a potential goal, we also predict the type of victim to be triaged next, which helps us identify the agent’s strategy or long term behavior. For example, we observed that some players prioritize triaging yellow victims because they are worth more points and expire sooner, while some players are more opportunistic, triaging victims in the order they appear in their field of view.

Note that the next victim to be triaged may not be in the current area that the player is in. Thus, we need to leverage information from both the high and low resolution representations to make this prediction, making it an important output that takes advantage of our multi-resolution architecture.

3.4 Architecture

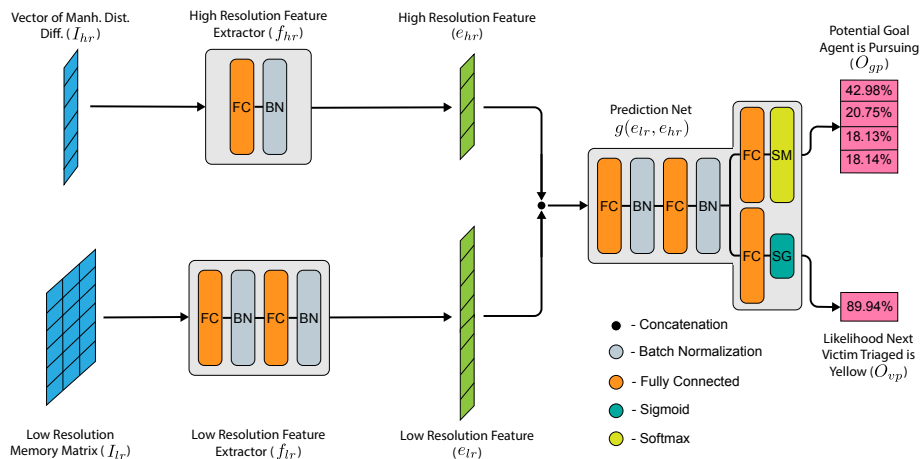


Fig. 5. This is our network architecture. Our inputs are fed into features extractors for each resolution and then those extracted features are concatenated and fed into the prediction net which produces our goal and victim type predictions. The values shown for O_{gp} and O_{vp} are taken from the example in Fig. 4 for illustrative purposes.

The architecture of the model is shown in Figure 5. First, the information from the high and low resolution representations are used as inputs. The high-resolution input I_{hr} is a vector of Δ_{MD} values, one for each goal. The low-resolution input I_{lr} is the memory matrix described earlier. The corresponding features $e_{hr} = f_{hr}(I_{hr})$ and $e_{lr} = f_{lr}(I_{lr})$ are extracted by the feature extractor networks f_{hr} and f_{lr} , respectively. Then, these two features from the two different resolutions are concatenated and fed into the prediction net g . The next goal and victim type to be triaged predictions O_{gp} and O_{vp} take the form of estimating the two probabilistic outputs with $g(e_{lr}, e_{hr})$. Since the inputs consider state differences rather than the entire state, the size of the input observation space is significantly reduced, thereby reducing the training difficulty of our deep learning model. We use a fully connected (FC) layer combined with a batch normalization layer as a basic building block for our three neural networks. The output FC layers in the prediction network ($g(e_{lr}, e_{hr})$) are passed through softmax and sigmoid functions to obtain the probabilities of the agent’s goal (O_{gp}) and the likelihood that the next victim is triaged (O_{vp}), respectively.

High-Resolution Input Similar to the setting of the BToM [3], we infer the probability of pursuing a goal. As shown in Figure 4, we compute the quantity Δ_{MD} , defined as follows:

$$\Delta_{\text{MD}}(g, m) = D(x_i^m, x_g) - D(x_f^m, x_g) \quad (1)$$

where x_i^m and x_f^m are the initial and final positions of the agent computed with respect to a window of the past m ‘move’ primitive actions, x_g is the location of the goal g for which Δ_{MD} is being calculated, and $D(a, b)$ is the Manhattan distance between locations a and b . We found that setting $m = 6$ to be the best fit choice, which still gives real-time predictions, while also handling some noise in the agent’s actions. See Table 4 for a comparison of results with different values of m .

Low-Resolution Input As shown in Figure 2, we record the victim status and area visitation status of each area in a matrix and use it as an input to the proposed model. This input helps us extract long-term historical information to form memory and facilitate the extraction of high-level features (long term strategies) as a prior to human behavior predictions.

4 Evaluation

Our model is trained in an end-to-end manner via supervised learning using an Nvidia V100S GPU and the Adam optimization algorithm [27]. We calculate the softmax cross entropy loss for goal prediction and the binary cross entropy loss for victim type prediction. The training loss L_{total} is the sum of the goal prediction loss L_{gp} and the victim type loss L_{vp} as seen in eq. 2, where the victim type loss weight, W , is given in Table 2, along with the rest of the training hyperparameters after tuning.

$$L_{\text{total}} = L_{\text{gp}} + W * L_{\text{vp}} \quad (2)$$

Figure 4 illustrates how our proposed model works. As shown in Fig. 1, in the room that the agent searched just prior to the room that it is currently in, the agent only triaged the yellow victim and left the two green victims, which hints that that the agent is likely following a strategy that prioritizes rescuing all the yellow victims first. Our model encodes this behavior as prior knowledge and predicts that the probability that the next victim to be triaged will be yellow is ≈ 0.9 .

Without a prior about the rescue strategy we may naively expect that the agent will move from G2 to G3 or G4 (i.e., to the next closest victim) with a high probability. In contrast, our model predicts that the most likely next short-term goal is the room’s exit, with a probability of ≈ 0.43 . In Figure 6 (similar to Fig. 4), the same player finally chose to leave after finding there is no yellow victims in this room. The probability of the agent returning to G1 to try and find a yellow victim to triage next can be seen to increase from about 0.90 to 0.95.

Table 2. Hyperparameters for our model training.

Hyperparameter	Value
Learning rate	0.001
Low resolution feature size	64
High resolution feature size	4
Hidden size for prediction net	64
Batch size	16
Random seed	0
Victim type loss weight (W)	0.3

This demonstrates that our model can learn about high-level strategies that a player is following, and can also detect instantaneous changes in the short-term goals of human players.

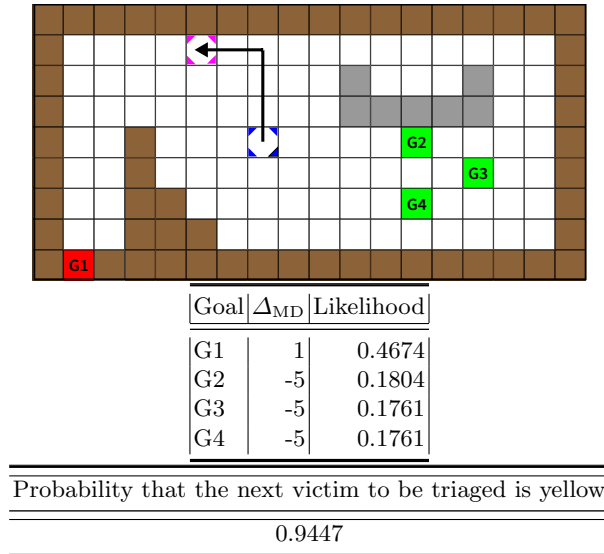


Fig. 6. The high resolution representation at a later time than the example shown in Fig. 4. Here we see the probabilities of the agent heading to goal G1, and that the next victim triaged will be yellow are increasing, showing that our model is correctly predicting the agent’s goals in real-time, in addition to showing our prediction at an earlier timestep was correct.

Table 3. Results for 6-fold cross-validation for our approach and two baselines based on high-resolution inputs. In the first method, we encode the high resolution input as the destination locations of the agent’s most recent six ‘move’ actions. For the second method, we concatenate the high resolution input vector I_{hr} with an integer representing which area the agent is in. We find that our multi-resolution approach significantly outperforms the baselines that only use high resolution inputs.

Model - Cross Val.	Easy		Medium		Hard	
	Goal Acc.	Vic. Acc.	Goal Acc.	Vic. Acc.	Goal Acc.	Vic. Acc.
High Res. (Locations)	0.6313	0.7060	0.6232	0.6874	0.6031	0.6838
High Res. (Δ_{MD}^i)	0.6526	0.7315	0.6412	0.7037	0.6251	0.6881
High + Low Res.	0.7208	0.9008	0.7146	0.8803	0.6780	0.8881

In Table 3, we compare our multi-resolution method to two baseline approaches based solely on high-resolution information³. The first baseline uses the 2D coordinates of the destination cells of the six most recent ‘move’ actions as the input. The second baseline considers the high-resolution input based on Δ_{MD} and includes only a small portion of the information from the low-resolution representation. Specifically, since the current area cannot be encoded if only Δ_{MD} is considered, we encode each area with a unique integer and append this integer to the input vector I_{hr} .

We have 66 trials for each difficulty level, and use a 6-fold cross-validation procedure to evaluate our model⁴. As shown in Table 3, we see that the baseline using Δ_{MD} performs better than the baseline that uses only the past six destination cells of the agent’s ‘move’ actions, and our approach that uses both high and low resolution information outperforms both the baselines. Compared to using location information alone, using Δ_{MD} (or more specifically, a vector of Δ_{MD} values, one for each goal, i.e., I_{hr}) as an input can lead to better features being extracted, thus improving prediction accuracy. Our proposed method based on the combination of high and low-resolution information allows our model to effectively learn the relationship between features at multiple resolutions in the data, further improving the accuracy of behavior prediction.

We also investigated the sensitivity of our approach to the choice of the parameter m (the number of moves in our window when we compute $\Delta_{MD}(m, g)$). The results are shown in Table 4. The performance of our proposed method is not overly sensitive to the number of moves, and thus we choose $m = 6$ after comprehensively considering the results for the three tasks.

³ We do not compare with an approach based solely on low-resolution information, as it would be not be sufficient to differentiate between multiple short-term goals within a single area/node

⁴ We evaluate the accuracy of the victim type prediction only in the first five minutes of each trial because yellow victims expire after five minutes, leaving only green victims to triage

Table 4. Results for 6-fold cross-validation for our approach in which the high resolution inputs are based on different numbers of ‘move’ actions.

last m moves	Easy		Medium		Hard	
	Goal Acc.	Vic. Acc.	Goal Acc.	Vic. Acc.	Goal Acc.	Vic. Acc.
3	0.7181	0.9037	0.7071	0.8816	0.6712	0.8857
6	0.7208	0.9008	0.7146	0.8803	0.6780	0.8881
12	0.7151	0.9001	0.7118	0.8835	0.6801	0.8845

5 Conclusion

In this paper, we proposed a real-time human behavior prediction model that uses multi-resolution features. In the high-resolution input, the model observes the Manhattan distance difference between the agent and each potential goal during recent behavior, which is robust to obtain the agent’s short-term intention. The low-resolution historical state matrix effectively organizes the long-term memory and helps the model extract the high-level feature. In addition, the supervised learning-based training provides a straightforward and automatic way to organize and learn the internal correlations from the human subjects data. After training, the experimental results demonstrated that our method is robust and accurate at effectively utilizes prior knowledge to predict human behavior.

References

1. Seeber, I., Bittner, E., Briggs, R. O., De Vreede, T., De Vreede, G.-J., Elkins, A., . . . Others.: Machines as teammates: A research agenda on AI in team collaboration. *Information & management*, **57**(2), 103174 (2020).
2. Rabinowitz, N., Perbet, F., Song, F., Zhang, C., Eslami, S. M. A. and Botvinick, M.: Machine Theory of Mind. *Proceedings of the 35th International Conference on Machine Learning*, 4218–4227. (July 2018).
3. Baker, C. L., Jara-Ettinger, J., Saxe, R., and Tenenbaum, J. B.: Rational quantitative attribution of beliefs, desires and percepts in human mentalizing. *Nature Human Behaviour*, **1**(4), 0064 (2017).
4. Wu, Y., Baker, C. L., Tenenbaum, J. B., and Schulz, L. E.: Rational inference of beliefs and desires from emotional expressions. *Cognitive science*, **42**(3), 850–884 (2018).
5. Galescu, L., Teng, C. M., Allen, J., and Perera, I.: Cogent: A Generic Dialogue System Shell Based on a Collaborative Problem Solving Model. *Proceedings of the 19th Annual SIGdial Meeting on Discourse and Dialogue*, 400–409. (July 2018).
6. Allen, J. F., Bahkshandeh, O., de Beaumont, W., Galescu, L., and Teng, C. M.: Effective Broad-Coverage Deep Parsing. *Proceedings of the Thirty-Second AAAI Conference on Artificial Intelligence, (AAAI-18)*, 4776–4783 (2018).
7. Perera, I., Allen, J., Teng, C. M., and Galescu, L.: Building and Learning Structures in a Situated Blocks World Through Deep Language Understanding. *Proceedings of the First International Workshop on Spatial Language Understanding*, 12–20. doi:10.18653/v1/W18-140 (June 2018).

8. Zhao, R., Papangelis, A., and Cassell, J.: Towards a Dyadic Computational Model of Rapport Management for Human-Virtual Agent Interaction. In T. W. Bickmore, S. Marsella, and C. L. Sidner, Proceedings of 14th International Conference of Intelligent Virtual Agents, 514–527. doi:10.1007/978-3-319-09767-1_6 (2014).
9. Zhao, R., Sinha, T., Black, A. W., and Cassell, J.: Socially-Aware Virtual Agents: Automatically Assessing Dyadic Rapport from Temporal Patterns of Behavior. Proceedings of the 16th International Conference of Intelligent Virtual Agents, 218–233. doi:10.1007/978-3-319-47665-0_2 (2016).
10. Huang, L., Freeman, J., Cooke, N., Buchanan, V., Wood, M. D., Freiman, M., ... Demir, M.: ASIST Experiment 1 Study Preregistration. doi:10.17605/OSF.IO/ZWAU (December 2020).
11. Zhi-Xuan, T., Mann, J. L., Silver, T., Tenenbaum, J., and Mansinghka, V.: Online Bayesian Goal Inference for Boundedly Rational Planning Agents. Proceedings of Annual Conference on Neural Information Processing Systems 2020 (2020).
12. Jara-Ettinger, J., Schulz, L. E., and Tenenbaum, J. B.: The Naïve Utility Calculus as a unified, quantitative framework for action understanding. *Cognitive Psychology*, **123**, 101334. doi:10.1016/j.cogpsych.2020.101333 (2020).
13. Baker, C. L., Saxe, R., and Tenenbaum, J. B.: Bayesian Theory of Mind: Modeling Joint Belief-Desire Attribution. Proceedings of the 33th Annual Meeting of the Cognitive Science Society (2011).
14. Ng, A. Y., and Russell, S. J.: Algorithms for Inverse Reinforcement Learning. Proceedings of the 17th International Conference on Machine Learning (ICML 2000), 663–670, (2000).
15. Abbeel, P. and Ng, A. Y.: Apprenticeship learning via inverse reinforcement learning. Proceedings of the 21 International Conference (ICML 2004), doi:10.1145/1015330.101543 (2004).
16. Ramachandran, D., and Amir, E.: Bayesian Inverse Reinforcement Learning. Proceedings of the 20th International Joint Conference on Artificial Intelligence, 2586–2591 (2007).
17. Hadfield-Menell, D., Dragan, A. D., Abbeel, P., and Russell, S. J.: Cooperative Inverse Reinforcement Learning. CoRR, (2016).
18. Brown, D. S., and Niekum, S.: Deep Bayesian Reward Learning from Preferences. CoRR, (2019).
19. Michini, B., and How, J. P.: Improving the efficiency of Bayesian inverse reinforcement learning. Proceedings of IEEE International Conference on Robotics and Automation, 3651–3656. doi:10.1109/ICRA.2012.622524 (2012).
20. Ramírez, M., and Geffner, H.: Plan Recognition as Planning. Proceedings of the 21st International Joint Conference on Artificial Intelligence, 1778–1783, (2009).
21. Ramírez, M., and Geffner, H.: Probabilistic Plan Recognition Using Off-the-Shelf Classical Planners. Proceedings of the 24th AAAI Conference on Artificial Intelligence, (2010).
22. Sohrabi, S., Riabov, A. V., and Udrea, O.: Plan Recognition as Planning Revisited. Proceedings of the 25th International Joint Conference on Artificial Intelligence, 3258–3264 (2016).
23. Höller, D., Bercher, P., Behnke, G., and Biundo, S.: Plan and Goal Recognition as HTN Planning. Proceedings of the Workshops of the 32th AAAI Conference on Artificial Intelligence, 607–613 (2018).
24. Kaminka, G. A., Vered, M., and Agmon, N.: Plan Recognition in Continuous Domains. Proceedings of the 32th AAAI Conference on Artificial Intelligence, 6202–6210 (2018).

25. Vered, M., Pereira, R. F., Magnaguagno, M. C., Meneguzzi, F., and Kaminka, G. A.: Online Goal Recognition as Reasoning over Landmarks. Proceedings of the Workshops of the 32th AAAI Conference on Artificial Intelligence, 638–645 (2018).
26. Guo, Y., Jena, R., Hughes, D., Lewis, M., and Sycara, K.: Transfer Learning for Human Navigation and Triage Strategies Prediction in a Simulated Urban Search and Rescue Task. Proceedings of 30th IEEE International Conference on Robot and Human Interactive Communication 784–791 (August 2021).
27. Kingma, D. P., and Ba, J.: Adam: A Method for Stochastic Optimization. Proceedings of the 3rd International Conference on Learning Representations, (2015).